Agric Res J **60** (5) : 740-745, *October* 2023
DOI No. 10.5958/2395-146X.2023.00105.9

NUMERICAL EVALUATION OF IMPROVED SOLAR DRYER FOR AGRICULTURAL APPLICATIONS

Mohit Singla[1*], V S Hans[2] and Sukhmeet Singh[2]

[1]Department of Renewable Energy Engineering; [2]Department of Mechanical Engineering
Punjab Agricultural University, Ludhiana-141004, Punjab

ABSTRACT

In the present work, performance of solar dryer having evacuated tube collector was enhanced by artificial roughness with circular rib for agricultural applications. The influence of roughness geometry parameters i.e. relative roughness pitch (P/e) of 12 and relative roughness height (e/D_h) of 0.057 on Nusselt number and friction factor has been investigated. Reynolds number considered for investigation varied from 2500 to 8000. Rughened solar evacuated tube collector performed better than smooth solar evacuated tube collector. Nusselt number augments with the increase in Reynolds number while friction factor shows an opposite trend with increase in Reynolds number. Maximum enhancement ratio of Nusselt number and friction factor is 1.54 and 2.43, respectively, obtained at Reynolds number of 8000. The value of thermo-hydraulic performance parameter for circular rib roughened solar evacuated tube collector varied between 1.09 - 1.15 over the entire range of Reynolds number.

Keywords: Artificial roughness, Evacuated tube collector, Friction factor, Nusselt number, Reynolds number, Solar dryer

A solar collector is an integral part of solar thermal systems and is commonly utilized for various applications such as air and water heating, space heating and cooling, cooking, and crop drying (Bansal, 1999). In conventional solar air heating systems, flat plate collector is commonly used to absorb, convert and transfer solar radiations to the air flowing through it (Belusko *et al*., 2008). However, flat plate collectors have deprived thermal efficiency due to poor convective heat transfer coefficient between absorber plate and air. Formation of heat resistive laminar sub-layer underside the absorber is the major cause of low convective heat transfer coefficient (Hans *et al*., 2009; Hans *et al*., 2017; Gill *et al*., 2017). Number of methods has been investigated by the researchers to improve thermal performance of solar air heaters but artificial roughness has found to be the most effective method as it breaks the laminar sub-layer, creates turbulence in flow region without disturbing core flow (Hans *et al*., 2010). Employing the rib roughness has negative effect on heat transferring surface with significant increase in pumping power requirements because of increased friction losses (Singh *et al*., 2011; Singh and Singh, 2017). A number of investigations have been carried out to study the influence of various shapes and arrangement of rib on heat transfer in solar air heater duct such as transverse ribs (Prasad and Saini, 1988), inclined rib (Gupta *et al*., 1997), arc shaped rib (Saini and Saini, 2008) and V-shaped rib (Momin *et al.*, 2002). A significant enhancement in thermo-hydraulic performance has observed because of increased turbulence in the flow region. Other geometries also have profound effect on heat transfer include broken transverse rib (Sahu and Bhagoria, 2005), multiple V ribs (Hans *et al.*, 2010), broken arc rib (Hans *et al*., 2017), discrete V-shaped rib (Karwa *et al*., 2003) Wedge shaped rib (Bhagoria *et al*., 2002) and S-shaped rib (Kumar *et al.*, 2017).

Recently some investigators used Computational Fluid Dynamics (CFD) analysis to determine the influence of roughness geometry parameters on thermal performance of roughened flat plate solar air heaters (Bauri *et al*., 2021; Yadav *et al.*, 2021; Misra *et al*., 2020;Singh *et al*., 2015). However, the focus of all the above stated investigations was to enhance the convective heat transfer coefficient between air and absorber without paying any attention to reduction in conductive and convective losses. In order to overcome the conductive and convective losses, solar evacuated tube collector was developed (Aranovitch, 1981). Thermal performance of evacuated tube collectors, in comparison to flat plate collectors, is quite high and feasibly used in forced circulation solar dryers to have high operating temperatures. A large capacity forced circulation dryer for drying of agricultural produce (turmeric, chilli, ginger, garlic, bitter gourd etc.) and herbs (amla, giloy, morianga leaves, lemon grass, harad etc.) has been developed. The forced circulation solar dryer consists of a greenhouse, an evacuated tube collector solar air heater and a tray rack having

*Corresponding author : mohit-sree@pau.edu
Date of receipt: 01.08.2023, Date of acceptance: 30.08. 2023

trays stacked in vertical for optimum utilization of space. However, the collector area required for such type of drying system is large and substantial space is occupied by the collectors. Moreover, there is a need to improve the thermal performance of solar evacuated tube collector so as to enhance the drying rate to achieve faster drying of the products. Therefore, it becomes imperative to increase the convective heat transfer coefficient between air and absorber with the application of heat transfer enhancement techniques.

Various studies have reported the application of circular rib in flat plate solar air heaters for heat transfer enhancement. It has been seen that no study was carried out on application of artificial roughness in evacuated tube collector solar air heater for heat transfer enhancement. Therefore, present investigation has been carried out using CFD to analyze heat transfer and friction characteristics of solar evacuated tube collector roughened artificially with circular rib of uniform cross-section with relative roughness pitch (P/e) and height (e/D) as 12 and 0.057 respectively. Thermo-hydraulic performance of roughened evacuated tube collector has been also evaluated.

MATERIALS AND METHODS

A 3-dimensional solar evacuated tube collector has a length, diameter and hydraulic diameter as 1800 mm, 43 mm and 28 mm, respectively. Tube is split in two parts vertically and roughened side is uniformly heated with 1000 W/m^2. The circular rib of uniform cross section is employed to the heat transferring surface to create artificial roughness. In the present investigation, roughness geometry parameters considered were relative roughness height (e/D_h) and relative roughness pitch (P/e) having value of 0.057 and 12 respectively. Reynolds number varied from 2500 to 8000.

Singla *et al*. (2022) compared the numerically determined values with those determined by using equation (1), mean absolute deviance in Nusselt number for different turbulence models (Standard k-ε with enhanced wall treatment, Standard k-ω, RNG k-ε with enhanced wall treatment and standard wall function, SST (Standard and shear stress transport) k-ω and Realizable k- ε with enhanced wall treatment under periodic and non-periodic flow conditions. It was found clear that turbulence model RNG k-ε with enhanced wall treatment under periodic flow conditions showed least mean absolute deviance of 18.45% in Nusselt number values. Therefore, in this numerical analysis, RNG k-ε with enhanced wall treatment model has been used under periodic flow conditions.

$$Nu=\frac{\left(\frac{f}{2}\right)(Re-1000)Pr}{1+12.7\left(\frac{f}{2}\right)^{0.5}\left(Pr^{2/3}-1\right)}\ (1+(\frac{D}{L})^{\frac{2}{3}})(\frac{\mu_b}{\mu_w})^{0.14}\ (1-0.14\ (\frac{D_1}{D_2})^{0.6} \text{ for } 2300 < Re < 1000000 \quad (1)$$

In the above equation 'f' represents fanning friction which is determined by using following empirical correlation (Filonenko, 1954):

$$f=0.25\ (1.82 \log_{10}Re - 1.64)^{-2} \quad (2)$$

Under this analysis, one pitch length of 19.2 mm was modeled in ANSYS design Modeler 15.0 and inlet periodic conditions were applied to flow only. Conservations equations were worked out by applying finite volume based numerical method (Raj *et al*., 2017). Inlet boundary conditions were evaluated from Reynolds number, as mass flow rate. Convergence limit of 10^{-10} for residual of energy equation and 10^{-5} for continuity, velocity, turbulence kinetic energy and turbulence dissipation equations were taken. The air flow in solar evacuated tube collector is considered to be steady, fully developed and turbulent.

Grid generation for the periodic flow domain was done in ANSYS Meshing Component as shown in Fig. 1. Initially, results were obtained by using coarse mesh but subsequently mesh was refined using gradient adaption with a maximum fluctuation of 20% in each parameter viz. temperature, pressure, velocity, turbulence intensity and wall shear stress (Singla *et al.,* 2022; Singla *et al.,* 2023). It is shown in Table 1 that after refining the mesh, percent deviation in Nusselt number is almost negligible (<1%). Gradient adaptions were conducted to make the results as grid independent.

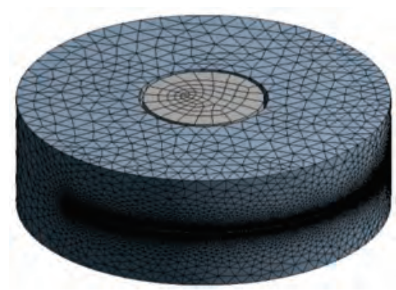

Fig. 1. Mesh on period flow domain

RESULTS AND DISCUSSION

Heat transfer characteristics

Influence of circular rib on heat transfer characteristics of a solar evacuated tube collector was determined. The variation of Nusselt number with Reynolds number for roughened and smooth solar evacuated tube is shown in Fig. 2. It is clearly seen from the Fig. 2 that the value of Nusselt number augments as the Reynolds number increased from 2500 to 8000. This augmentation in Nusselt number is attributed to the fact that dissipation rate, turbulent kinetic energy and severity of the turbulence increased with Reynolds number increase (Singh *et al.,* 2015; Singla *et al*., 2022; Singla *et al.,* 2023). Nusselt number increases from 16.41 to 35.78 with the increment of Reynolds number

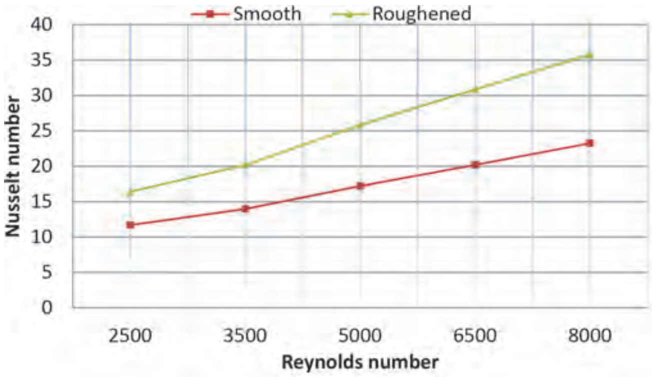

Fig. 2. Variation in Nusselt number for circular rib at different Reynolds number

from 2500 to 8000. Maximum value of Nusselt number is obtained at Reynolds number of 8000.

In fig. 3 streamlines are drawn at mid-plane to view the flow behavior around the rib. Area of flow recirculation zone is compared for Reynolds number of 2500 and 8000. It is clearly spotted in Fig. 3 (a) that the flow recirculation area, represents the low transfer zone at lower Reynolds number is large. As the Reynolds number increased from 2500 to 8000 area of the flow recirculation zone reduced, resulting in more contact of air with absorber which leads to enhancement of Nusselt number (Singh and Singh, 2017). In comparison to the smooth evacuated tube, maximum enhancement of 1.54 times in Nusselt number was observed at Reynolds number value of 8000.

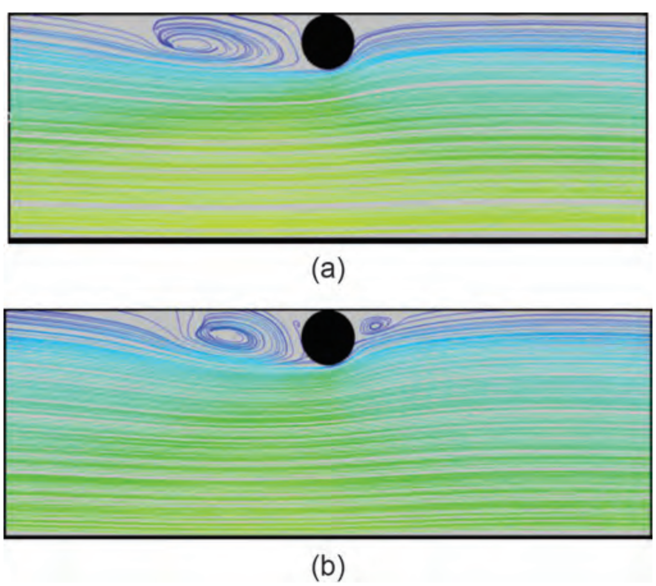

Fig. 3. Streamlines on central plane normal to rib roughness at Reynolds number of (a) 2500 (b) 8000

Friction factor characteristics

Application of circular rib creates obstacle to flow resulting in increase of turbulence intensity around the rib which leads to increase in Nusselt number and frictional losses. These frictional losses have been estimated from the pressure drop across the solar evacuated tube collector using the Darcy's equation (3).

$$f = \frac{2\Delta P D_h}{4\rho L v^2} \tag{3}$$

The variation of pressure loss with Reynolds number for smooth and roughened solar evacuated tube collector is shown in Fig. 4. Turbulence intensity increases with the increase in Reynolds number from 2500 to 8000 resulting in increase in pressure drop at higher value of Reynolds number. Fig. 5 shows the static pressure contours and development of drag around the rib which indicates that air particles are compressed at upstream end of the rib whereas these air particles are spaced out at downstream end. It is clearly seen from Fig. 5 (a) that at lower Reynolds number, pressure loss is less due to smaller reattachment length of flow whereas pressure loss increases with the increase in Reynolds number (Fig. 5 (b)).

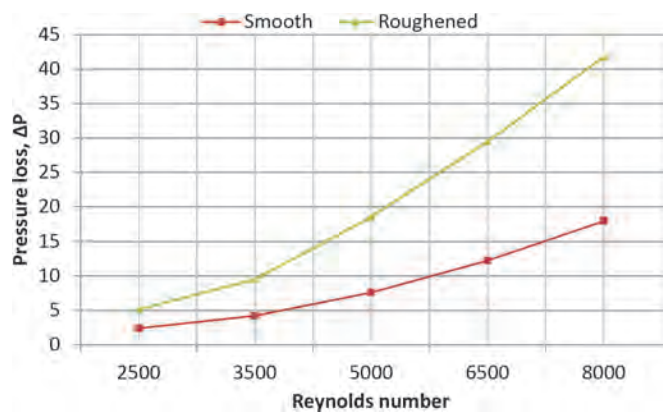

Fig. 4. Variation in pressure loss for circular rib at different Reynolds number

Pressure loss in roughened solar evacuated tube collector is more as compared to smooth solar evacuated tube collector because of flow separation and reattachment due to presence ribs which pushes the flow in backward direction resulting in higher pressure loss. However, friction factor reduces as the Reynolds number augments from 2500 to 8000 as shown in Fig. 6. This reduction is due to the fact that velocity factor dominates more as comparison to pressure drop in evaluating the friction factor from the Eq (3). Friction factor reduces from 0.0155 to 0.0124 as the Reynolds number augments from 2500 to 8000. Maximum enhancement in friction factor was 2.43 times at Re = 8000 as compared to smooth solar evacuated tube collector.

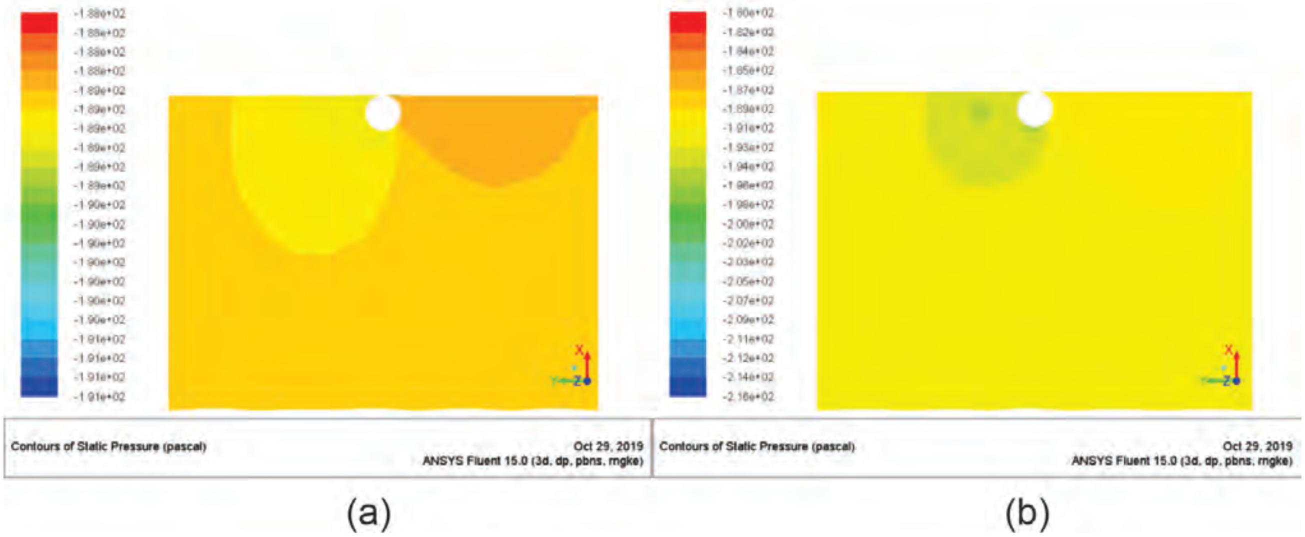

Fig. 5. Static pressure contours on central plane normal to rib roughness at Reynolds number of (a) 2500 (b) 8000

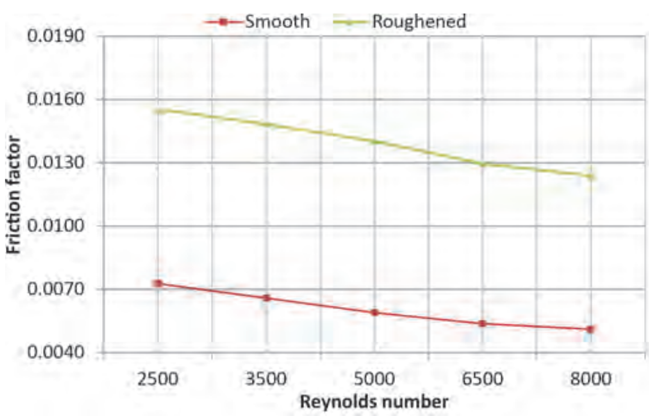

Fig. 6. Variation in friction factor for circular rib at different Reynolds number

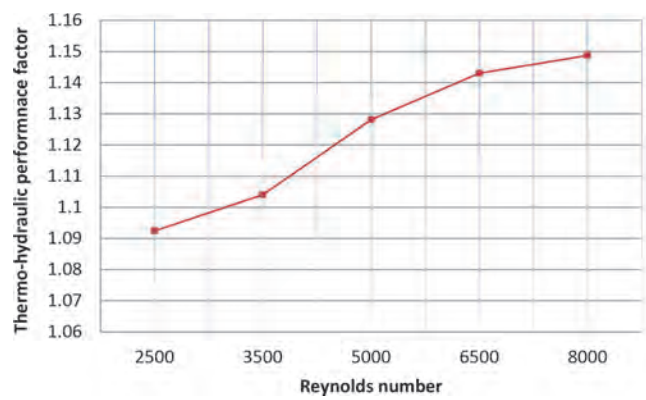

Fig. 7. Variation in thermo-hydraulic performance factor for circular rib at different Reynolds number

Thermo-hydraulic performance factor

The overall performance of solar air heaters is estimated in terms of thermo-hydraulic performance factor given by Maradiya *et al.* (2018).

$$\eta = \frac{{Nu_r}/{Nu_s}}{\left({f_r}/{f_s}\right)^{1/3}} \tag{4}$$

Fig. 7 shows the thermo-hydraulic performance factor (THPF) of circular rib roughened evacuated tube collector for Reynolds number range of 2500-8000. It is observed that thermo-hydraulic performance factor is more than unity which indicates the benefit of applying the circular rib. The THPF enhances with the increment in Reynolds number varies from 1.09-1.15 and maximum value is found corresponds to Reynolds number value of 8000. It is due to the fact that Nusselt number augmentation ratio increases resulting in increase in THPF.

In the present study, CFD analysis was conducted to study the influence of roughness geometry parameters for different values of Reynolds number on heat transfer and friction characteristics of rib roughened solar evacuated tube collector. With the increase in Reynolds number, Nusselt number increases whereas friction factor decreases. Nusselt number and friction factor of roughened solar evacuated tube collector is found to be more as compared to smooth solar evacuated tube collector. Maximum augmentation in Nusselt number and friction factor for roughened solar evacuated tube collector is 1.54 and 2.43 over smooth solar evacuated tube collector. The thermo-hydraulic performance factor varies from 1.09-1.15 for the entire range of Reynolds number investigated which indicates considerable benefit of applying circular rib roughness in solar evacuated tube collector.

Table 1. Percent deviation in Nusselt number after several gradient adaptions at P/e = 12, e/D= 0.057 and Re = 8000

Adaptions	Number of Elements	Nusselt number	Deviation in Nusselt number (%)
Before adaption	1000833	36.80	-
Temperature	1297829	36.57	0.63
Pressure	1422338	36.38	0.52
Velocity	1446558	36.22	0.44
Turbulence intensity	1467495	35.89	0.91
Wall shear stress	1485877	35.78	0.31

Nomenclature

D hydraulic diameter of tube, mm
e rib height, mm
e/D_h relative roughness height
L length of tube, mm
P pitch, mm
P/e relative roughness pitch
ΔP pressure drop across the tube, Pa
v velocity, m/s
ρ density of air, Kg/m^3

Authors' contribution

Conceptualization of research work and designing of experiments(VS, SS, MS); Execution of field/lab experiments and data collection(MS, VS, SS); Data analysis and interpretation of results(MS, VS, SS); Preparation of manuscript(MS, VS, SS).

LITERATURE CITED

Aranovitch E 1981. Performance of solar energy converters: Thermal collectors and photovoltaic cells. In *Solar Thermal Collectors,* Beghi G (ed.). Springer Dordrecht, Italy, pp.11-18.

Bansal N K 1999. Solar air heater applications in India. *Renewable Energy* **16**: 618–23.

Bauri S K and Prasad A K 2021. A CFD-based thermal analysis of solar air heater duct artificially roughened with 'S' shape ribs on absorber plate. *AIP Conference Proc* **2341**: 1-19.

Belusko M, Saman W and Bruno F 2008. Performance of jet impingement in unglazed air collectors. *Solar Energy* **82**: 389-98.

Bhagoria J L, Saini J S and Solanki S C 2002. Heat transfer coefficient and friction factor correlations for rectangular solar air heater duct having transverse wedge shaped rib roughness on the absorber plate. *Ren Energy* **25**: 341-69.

Filonenko G K 1954. Hydraulic resistance in pipes. *Teploenergetika* **1**: 40-44.

Gill R S, Hans V S, Saini J S and Singh S 2017. Investigation on performance enhancement due to staggered piece in a broken arc rib roughened solar air heater duct. *Ren Energy* **104**:148-62.

Gupta D, Solanki S C and Saini J S 1997. Thermohydraulic performance of solar air heaters with roughened absorber plates. *Solar Energy* **61**: 33-42.

Hans V S, Gill R S and Singh S 2017. Heat transfer and friction factor correlations for a solar air heater duct roughened artificially with broken arc ribs. *Exp Thermal Fluid Sci* **80**: 77-89.

Hans V S, Saini R P, and Saini J S 2009. Performance of artificially roughened solar air heaters -A review. *Ren Sust Energy Rev* **13**: 1854-69.

Hans V S, Saini R P and Saini J S 2010. Heat transfer and friction factor correlations for a solar air heater duct roughened artificially with multiple v-ribs. *Solar Energy* **84**: 898-911.

Karwa R K 2003. Experimental studies of augmented heat transfer and friction in asymmetrically heated rectangular ducts with ribs on heated wall in transverse, inclined, v-continuous and v-discrete pattern. *Int Comm Heat and Mass Trans* **30**: 241-50.

Kumar K, Prajapati D and Samir S 2017. Heat transfer and friction factor correlations development for solar air heater duct artificially roughened with 'S' shape ribs. *Exp Thermal Fluid Sci* **82**: 249-61.

Maradiya C, Vadher J and Agarwal R 2018. The heat transfer enhancement techniques and their thermal performance factor. *Beni-Suef University J Basic and Appl Scie* **7**: 1-21.

Misra R, Singh J, Jain S K, Faujdar S, Agrawal M, Mishra A and Goyal P K 2020. Prediction of behavior of triangular solar air heater duct using V-down rib with multiple gaps and turbulence promoters as artificial roughness: A CFD analysis. *Intl J Heat and Mass Trans* **162**: 120376.

Momin A M E, Saini J S and Solanki S C 2002. Heat transfer and friction in solar air heater duct with v-shaped rib roughness on absorber plate. *Int J Heat and Mass Trans* **45**: 3383-96.

Prasad B N and Saini J S 1988.Effect of artificial roughness on heat transfer and friction factor in a solar air heater. *Solar Energy* **41**: 555-60.

Raj A K, Dileep K and Jayaraj S 2017. Solar ETC type water heaters- An analysis Based on CFD Packages. *Indian J Sci Technol* **10**: 1-8.

Sahu M M and Bhagoria J L 2005. Augmentation of heat transfer coefficient by using 90° broken transverse ribs on absorber plate of solar air heater. *Ren Energy* **30**: 2057-63.

Saini S K and Saini R P 2008. Development of correlations for Nusselt number and friction factor for solar air heater with roughened duct having arc-shaped wire as artificial roughness. *Solar Energy* **82**:1118–30.

Singh I and Singh S 2017. CFD analysis of solar air heater duct having square wave profiled transverse ribs as roughness elements. *Solar Energy* **162**: 442-53.

Singh S, Chander S and Saini J S 2011. Heat transfer and friction factor correlations of solar air heater ducts artificially roughened with discrete V-down ribs. *Energy* **36**: 5053-64.

Singh S, Singh B, Hans V S and Gill R S 2015. CFD (computational fluid dynamics) investigation on Nusselt number and friction factor of solar air heater duct roughened with non-uniform cross-section transverse rib. *Energy* **84**: 509-17.

Singla M, Hans V S and Singh S 2022. CFD analysis of rib roughened solar evacuated tube collector for air heating. *Ren Energy* **183**: 78-89.

Singla M, Hans V S and Singh S 2023. Fluid flow and heat transfer characteristics of artificially roughened evacuated tube collector. *Materials Today: Proc* **78**: 825-29.

Yadav A S, Shrivastava V, Sharma A and Dwivedi M K 2021. Numerical simulation and CFD-based correlations for artificially roughened solar air heater. *Materials Today: Proc* **47**: 2685-93.